

# High-order finite element modeling of M1-AWBS nonlocal electron transport

Milan, Vladimir, Philippe, Jean-Luc<sup>a</sup>

<sup>a</sup>*Université de Bordeaux - CNRS - CEA, CELIA, UMR 5107, F-33405 Talence, France*

---

## Abstract

*Keywords:* Nonlocal transport, Kinetics, MHD, High-order methods, FEM

---

## Contents

<b>1</b>	<b>M1 model</b>	<b>2</b>
1.1	AWBS Boltzmann transport equation . . . . .	2
1.2	M1-AWBS model . . . . .	2
<b>2</b>	<b>High-order finite element scheme</b>	<b>2</b>
2.1	Variational principle . . . . .	2
2.2	Semi-discrete formulation . . . . .	4
2.3	Explicit fully-discrete scheme . . . . .	5
2.4	Physical analysis of the diffusive asymptotics . . . . .	6
2.5	Implicit fully-discrete scheme . . . . .	7

## 1. M1 model

### 1.1. AWBS Boltzmann transport equation

Simplified Boltzmann transport equation of electrons relying on the use of AWBS collision-thermalization operator [1] reads

$$v\mathbf{n} \cdot \nabla f + \frac{q_e}{m_e} \left( \mathbf{E} + \frac{v}{c} \mathbf{n} \times \mathbf{B} \right) \cdot \nabla_{\mathbf{v}} f = \nu_e v \frac{\partial}{\partial v} (f - f_M). \quad (1)$$

### 1.2. M1-AWBS model

5 In order to eliminate the dimensions of the transport problem (1) the two moment model referred to as *M1-AWBS* is introduced

$$\nu_e v \frac{\partial}{\partial v} (f_0 - f_M) = v \nabla \cdot \mathbf{f}_1 + \frac{q_e}{m_e v^2} \mathbf{E} \cdot \frac{\partial}{\partial v} (v^2 \mathbf{f}_1), \quad (2)$$

$$\begin{aligned} \nu_e v \frac{\partial}{\partial v} \mathbf{f}_1 - \nu_t \mathbf{f}_1 &= v \nabla \cdot (\mathbf{A} f_0) + \frac{q_e}{m_e v^2} \mathbf{E} \cdot \frac{\partial}{\partial v} (v^2 \mathbf{A} f_0) \\ &\quad + \frac{q_e}{m_e v} \mathbf{E} \cdot (\mathbf{A} - \mathbf{I}) f_0 + \frac{q_e}{m_e c} \mathbf{B} \times \mathbf{f}_1, \end{aligned} \quad (3)$$

where the anisotropy-closure matrix takes the form

$$\mathbf{A} = \frac{1}{3} \mathbf{I} + \frac{|\mathbf{f}_1|^2}{2f_0^2} \left( 1 + \frac{|\mathbf{f}_1|^2}{f_0^2} \right) \left( \frac{\mathbf{f}_1 \otimes \mathbf{f}_1^T}{|\mathbf{f}_1|^2} - \frac{1}{3} \mathbf{I} \right), \quad (4)$$

which corresponds to the distribution function approximation

$$f = f_0 \frac{|\mathbf{M}_{(\mathbf{f}_1/f_0)}|}{4\pi \sinh(\mathbf{M}_{(\mathbf{f}_1/f_0)})} \exp(\mathbf{n} \cdot \mathbf{M}_{(\mathbf{f}_1/f_0)}), \quad (5)$$

where  $\mathbf{M}_{(\mathbf{f}_1/f_0)} \rightarrow 0$  when  $\mathbf{f}_1/f_0 \rightarrow \mathbf{0}$ .

## 2. High-order finite element scheme

### 2.1. Variational principle

First, the electro-magnetic scaling

$$\tilde{\mathbf{E}} = \frac{q_e}{m_e} \mathbf{E}, \quad \tilde{\mathbf{B}} = \frac{q_e}{m_e c} \mathbf{B}, \quad (6)$$

10 is defined in order to make the algebraic operations easier to follow. The general variational formulation of (2) and (3) constructed above the scalar (zero

moment) functional space represented by test functions  $\phi$  and the vector (first moment) functional space represented by test functions  $\mathbf{w}$  takes the form

$$\begin{aligned}\int_{\Omega} \phi \nu_e \frac{\partial f_0}{\partial v} &= \int_{\Omega} \phi \left( \mathbf{I} : \nabla \mathbf{f}_1 + \frac{1}{v} \tilde{\mathbf{E}} \cdot \frac{\partial \mathbf{f}_1}{\partial v} + \frac{2}{v^2} \tilde{\mathbf{E}} \cdot \mathbf{f}_1 + \nu_e \frac{\partial f_M}{\partial v} \right), \quad (7) \\ \int_{\Omega} \mathbf{w} \cdot \nu_e \frac{\partial \mathbf{f}_1}{\partial v} &= \int_{\Omega} \mathbf{w} \cdot \left( \nabla \cdot (\mathbf{A} f_0) + \frac{1}{v^2} \tilde{\mathbf{E}} \cdot (3\mathbf{A} - \mathbf{I}) f_0 \right. \\ &\quad \left. + \frac{1}{v} \tilde{\mathbf{E}} \cdot \frac{\partial}{\partial v} (\mathbf{A} f_0) + \frac{1}{v} \tilde{\mathbf{B}} \times \mathbf{f}_1 + \frac{\nu_t}{v} \mathbf{f}_1 \right). \quad (8)\end{aligned}$$

The corresponding discrete variational principal based on the method of finite elements then reads

$$\begin{aligned}\int_{\Omega} \phi \otimes \phi^T \nu_e d\Omega \cdot \frac{\partial \mathbf{f}_0}{\partial v} &= \int_{\Omega} \phi \otimes \left( \mathbf{I} : \nabla \mathbf{w}^T + \frac{2}{v^2} \tilde{\mathbf{E}}^T \cdot \mathbf{w}^T \right) d\Omega \cdot \mathbf{f}_1 \\ &\quad + \int_{\Omega} \phi \otimes \frac{1}{v} \tilde{\mathbf{E}}^T \cdot \mathbf{w}^T d\Omega \cdot \frac{\partial \mathbf{f}_1}{\partial v} + \int_{\Omega} \phi \otimes \phi^T \nu_e d\Omega \cdot \frac{\partial \mathbf{f}_M}{\partial v}, \quad (9)\end{aligned}$$

$$\begin{aligned}\int_{\Omega} \mathbf{w} \cdot \mathbf{w}^T \nu_e d\Omega \cdot \frac{\partial \mathbf{f}_1}{\partial v} &= - \int_{\Omega} (\mathbf{A} : \nabla \mathbf{w}) \phi^T d\Omega \cdot \mathbf{f}_0 \\ &\quad + \int_{\Omega} \mathbf{w} \cdot \frac{1}{v^2} (3\mathbf{A} - \mathbf{I}) \cdot \tilde{\mathbf{E}} \phi^T d\Omega \cdot \mathbf{f}_0 + \int_{\Omega} \mathbf{w} \cdot \frac{1}{v} \mathbf{A} \cdot \tilde{\mathbf{E}} \phi^T d\Omega \cdot \frac{\partial \mathbf{f}_0}{\partial v} \\ &\quad + \int_{\Omega} \mathbf{w} \cdot \left( \frac{1}{v} \tilde{\mathbf{B}} \times \mathbf{w}^T + \frac{\nu_t}{v} \mathbf{w}^T \right) d\Omega \cdot \mathbf{f}_1, \quad (10)\end{aligned}$$

where  $\phi$  is the finite vector of scalar bases functions,  $\mathbf{w}$  is the finite vector  
15 of vector bases functions,  $\Omega$  represents the computational domain, in principle 1D/2D/3D spatial mesh.

## 2.2. Semi-discrete formulation

In principle, only five following integrators need to be coded to provide a discrete representation (9) and (10), i.e.

$$\mathcal{M}_{(g)}^0 = \int_{\Omega} \phi \otimes \phi^T g \, d\Omega, \quad (11)$$

$$\mathcal{M}_{(g)}^1 = \int_{\Omega} \mathbf{w} \cdot \mathbf{w}^T g \, d\Omega, \quad (12)$$

$$\mathcal{D}_{(\mathbf{G})} = \int_{\Omega} \mathbf{G} : \nabla \mathbf{w} \otimes \phi^T \, d\Omega, \quad (13)$$

$$\mathcal{V}_{(g)} = \int_{\Omega} \mathbf{w} \cdot \mathbf{g} \otimes \phi^T \, d\Omega, \quad (14)$$

$$\mathcal{B}_{(g)} = \int_{\Omega} \mathbf{w} \cdot \mathbf{g} \times \mathbf{w}^T \, d\Omega. \quad (15)$$

The algebraic representation of the above mathematical objects, which form the basis for numerical discretization, reads

$$\phi = \begin{bmatrix} \phi_1 \\ \vdots \\ \phi_{N_0} \end{bmatrix}, \quad \mathbf{w} = \begin{bmatrix} w_{1,1} & \dots & w_{1,d} \\ \vdots & \ddots & \vdots \\ w_{N_1,1} & \dots & w_{N_1,d} \end{bmatrix}, \quad \mathbf{g} = \begin{bmatrix} g_1 \\ \vdots \\ g_d \end{bmatrix}, \quad \mathbf{G} = \begin{bmatrix} G_{1,1} & \dots & G_{1,d} \\ \vdots & \ddots & \vdots \\ G_{d,1} & \dots & G_{d,d} \end{bmatrix}, \quad (16)$$

where  $d$  is the number of spatial dimensions,  $N_0$  the number of degrees of freedom of scalar unknown  $\mathbf{f}_0$ , and  $N_1$  is the number of degrees of freedom of vector unknown  $\mathbf{f}_1$ .

Consequently, the discrete analog of M1-AWBS equations (2) and (3) can be written based on (9), (10) as

$$\mathcal{M}_{(\nu_e)}^0 \cdot \frac{\partial \mathbf{f}_0}{\partial v} - \mathcal{M}_{(\nu_e)}^0 \cdot \frac{\partial \mathbf{f}_M}{\partial v} = \mathcal{D}_{(\mathbf{I})}^T \cdot \mathbf{f}_1 + \frac{1}{v} \mathcal{V}_{(\tilde{\mathbf{E}})}^T \cdot \frac{\partial \mathbf{f}_1}{\partial v} + \frac{2}{v^2} \mathcal{V}_{(\tilde{\mathbf{E}})}^T \cdot \mathbf{f}_1, \quad (17)$$

$$\begin{aligned} \mathcal{M}_{(\nu_e)}^1 \cdot \frac{\partial \mathbf{f}_1}{\partial v} - \frac{1}{v} \mathcal{M}_{(\nu_t)}^1 \cdot \mathbf{f}_1 &= -\mathcal{D}_{(\mathbf{A})} \cdot \mathbf{f}_0 \\ &+ \frac{1}{v} \mathcal{V}_{(\mathbf{A} \cdot \tilde{\mathbf{E}})} \cdot \frac{\partial \mathbf{f}_0}{\partial v} + \frac{1}{v^2} \mathcal{V}_{((3\mathbf{A}-\mathbf{I}) \cdot \tilde{\mathbf{E}})} \cdot \mathbf{f}_0 + \frac{1}{v} \mathcal{B}_{(\tilde{\mathbf{B}})} \cdot \mathbf{f}_1, \end{aligned} \quad (18)$$

where the integrators (11), (12), (13), (14), (15) are used acting on appropriate functions  $\rho$ ,  $\nu_e$ ,  $\nu_t$ , vectors  $\tilde{\mathbf{E}}$ ,  $\tilde{\mathbf{B}}$ , and matrices  $\mathbf{A}$  and  $\mathbf{I}$ .

### 25 2.3. Explicit fully-discrete scheme

The easiest way to define a fully discrete scheme is to apply the explicit integration in time, e.g. RK4. Because of the use of different finite element spaces for zero and first moment, and a consequent difficulties of "mass" inversion, a modified two-step explicit scheme is used.

In the first step the time evolution of zero moment quantity  $\mathbf{f}_0$  is computed as

$$\left( \mathcal{M}_{(\nu_e)}^0 - \mathcal{M}_{\left(\frac{1}{v f_0^0} \tilde{\mathbf{E}}^T \cdot \mathbf{f}_1^n\right)}^0 \right) \cdot \frac{d\mathbf{f}_0}{dv}^* = \mathcal{D}_{(\mathbf{I})}^T \cdot \mathbf{f}_1^n + \frac{2}{v^2} \mathcal{V}_{(\tilde{\mathbf{E}})}^T \cdot \mathbf{f}_1^n + \mathcal{M}_{(\nu_e)}^0 \cdot \frac{\partial \mathbf{f}_M}{\partial v}, \quad (19)$$

where the actual evolution of  $\mathbf{f}_1$  has been redefined as similar to the time evolution of  $\mathbf{f}_0$  (compare (19) to (17)). Then, the actual computation of the time evolution of  $\mathbf{f}_1$  follows

$$\begin{aligned} \mathcal{M}_{(\nu_e)}^1 \cdot \frac{d\mathbf{f}_1}{dv} = & -\mathcal{D}_{(\mathbf{A})} \cdot \mathbf{f}_0^n + \frac{1}{v} \mathcal{V}_{(\mathbf{A} \cdot \tilde{\mathbf{E}})} \cdot \frac{d\mathbf{f}_0}{dv}^* \\ & + \frac{1}{v^2} \mathcal{V}_{((3\mathbf{A}-\mathbf{I}) \cdot \tilde{\mathbf{E}})} \cdot \mathbf{f}_0^n + \frac{1}{v} \mathcal{B}_{(\tilde{\mathbf{B}})} \cdot \mathbf{f}_1^n + \frac{1}{v} \mathcal{M}_{(\nu_t)}^1 \cdot \mathbf{f}_1^n. \end{aligned} \quad (20)$$

30 The superscript  $n$  stands for quantities from the previous level of velocity.

As can be seen in FIG. 2.4 we get a heat flux profile corresponding to temperature and density profiles computed by Laghos [2] in 1D and we have also double checked the numerical scheme in 2D and 3D, where apparently the flux profiles exhibit the same physical background. It is important to note, that  
35 the current implementation does not include neither electric or magnetic field  $(\tilde{\mathbf{E}}, \tilde{\mathbf{B}})$ .

It is worth mentioning, that the proposed discrete scheme (19) and (20) naturally obeys the CFL condition with respect to the mesh smallest cell size/mean-stopping-power, and consequently, we needed 8858 energy groups in 1D, 4348  
40 energy groups in 2D, and 10030 energy groups in 3D. This would make the hydro simulation to take more than 1000x longer than classical (SH) hydro.

#### 2.4. Physical analysis of the diffusive asymptotics

The BGK equation, valid for highly isotropic transport, represents the simplest form of the Boltzmann transport equation

$$\mathbf{n} \cdot \nabla f = \frac{(f_M - f)}{\lambda}, \quad (21)$$

where  $\lambda = \frac{v}{\nu_e} = \frac{av^4}{\rho}$  is the mean free path expressed as inverse of collisional frequency multiplied by particle velocity.

The Chapman-Enskog based small parameter ( $\lambda$ ) approximation  $f \approx f_0 + \lambda f_1 + O(\lambda^2)$  expressed as

$$\mathbf{n} \cdot \nabla (f_0 + \lambda f_1) = \frac{(f_M - (f_0 + \lambda f_1))}{\lambda}, \quad (22)$$

45 tells us, that

$$\begin{aligned} f_0 &= f_M, \\ f_1 &= -\mathbf{n} \cdot \nabla f_0 = -\mathbf{n} \cdot \nabla f_M, \end{aligned}$$

which means, that the localized approximation of the distribution function should behave as

$$f \approx f_M - \lambda \mathbf{n} \cdot \nabla f_M. \quad (23)$$

Consequently, one obtain a simple heat flux formula

$$\begin{aligned} \mathbf{q}_H &= \int_0^\infty \int_{4\pi} \frac{mv^3}{2} \mathbf{n} (f_M - \lambda \mathbf{n} \cdot \nabla f_M) v^2 d\mathbf{n} dv \\ &= -\frac{m}{2} \int_0^\infty \int_{4\pi} \mathbf{n} \otimes \mathbf{n} d\mathbf{n} \cdot \lambda \nabla f_M v^5 dv = -\frac{a}{\rho} \frac{m}{2} \int_0^\infty \frac{4\pi}{3} \nabla f_M v^9 dv \\ &= -\frac{a}{\rho} \frac{m}{2} \int_0^\infty \frac{4\pi}{3} \left( \frac{\partial f_M}{\partial \rho} \nabla \rho + \frac{\partial f_M}{\partial T} \nabla T \right) v^9 dv. \end{aligned} \quad (24)$$

$$\mathbf{q}_1 = \tilde{a}_1 T_1^\alpha \nabla T_1, \quad \mathbf{q}_0 = \tilde{a}_0 T_0^\alpha \nabla T_0,$$

where we keep  $\tilde{a}_1 = \tilde{a}_0 = \tilde{a}$  and  $\nabla T_1 = \nabla T_0 = \nabla T$  to be equal in every point of the computational domain. The ration of the fluxes than provides a very important information about flux nonlinearity

$$\frac{\mathbf{q}_1}{\mathbf{q}_0} = \frac{\tilde{a} T_1^\alpha \nabla T}{\tilde{a} T_0^\alpha \nabla T} = \left( \frac{T_1}{T_0} \right)^\alpha,$$

where the nonlinearity is better expressed as

$$\alpha = \frac{\log\left(\frac{\mathbf{q}_1}{\mathbf{q}_0}\right)}{\log\left(\frac{T_1}{T_0}\right)} \quad (25)$$

Finally, based on the simulation results of two runs corresponding to temperature  $T_0$  with the mean  $T = 1000$  executed as

```
mpirun -np 8 nth -p 5 -m data/segment01.mesh -rs 6 -tf 0.0 -ok 4 -ot 3
-vis -fa -print -Tmax 1050 -Tmin 950 -a0 1e12,
```

and to temperature  $T_1$  with the mean  $T = 1100$  executed as

```
mpirun -np 8 nth -p 5 -m data/segment01.mesh -rs 6 -tf 0.0 -ok 4 -ot 3
-vis -fa -print -Tmax 1150 -Tmin 1050 -a0 1e12,
```

we got the following numbers

$$\mathbf{q}_1 = 0.1782, \mathbf{q}_0 = 0.1406, T_1 = 1100, T_0 = 1000,$$

which provide the corresponding nonlinearity

$$\alpha = 2.486487132294661. \quad (26)$$

### 2.5. Implicit fully-discrete scheme

In order to formulate a fully-discrete scheme leaning on an implicit discretization of velocity, the equations (17) and (18) can be expressed with matrices as

$$\begin{aligned} \mathbf{M}_0 \cdot \frac{\partial \mathbf{f}_0}{\partial v} &= \mathbf{D}_0 \cdot \mathbf{f}_1 + \mathbf{E}_0^1 \cdot \frac{\partial \mathbf{f}_1}{\partial v} + \mathbf{E}_0^2 \cdot \mathbf{f}_1 + \mathbf{M}_0 \cdot \frac{\partial \mathbf{f}_M}{\partial v}, \\ \mathbf{M}_1 \cdot \frac{\partial \mathbf{f}_1}{\partial v} &= -\mathbf{D}_1 \cdot \mathbf{f}_0 + \mathbf{E}_1^1 \cdot \frac{\partial \mathbf{f}_0}{\partial v} + \mathbf{E}_1^2 \cdot \mathbf{f}_0 + \mathbf{B} \cdot \mathbf{f}_1 + \mathbf{M}_1^t \cdot \mathbf{f}_1, \end{aligned}$$

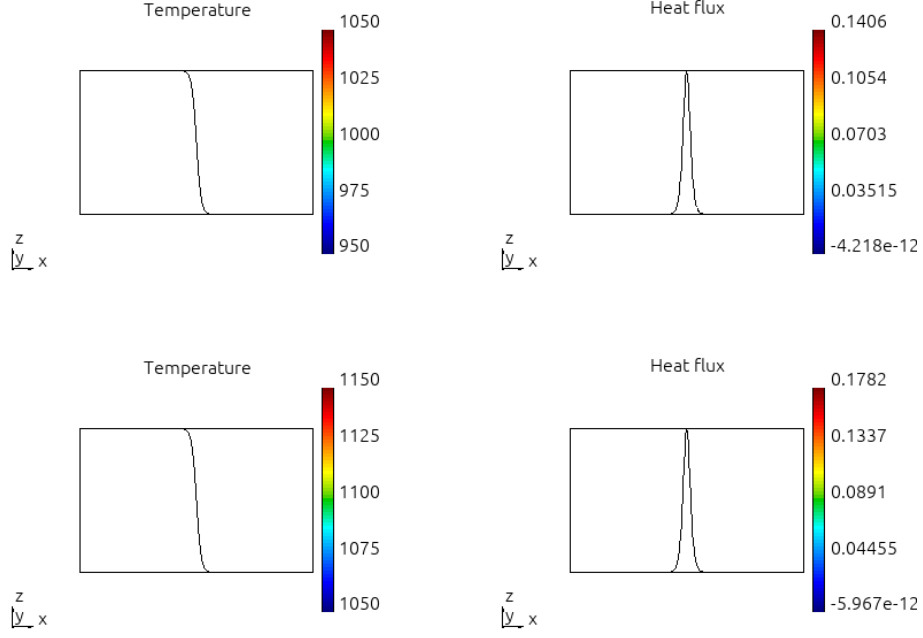


Figure 1: Problem 5 - AWBS nonlinearity check.

$$\begin{aligned}
\frac{d\mathbf{f}_0}{dv} &= \mathbf{M}_0^{-1} \cdot (\mathbf{D}_0 + \mathbf{E}_0^2) \cdot \left( \mathbf{f}_1^n + \Delta v \frac{d\mathbf{f}_1}{dv} \right) + \mathbf{M}_0^{-1} \cdot \mathbf{E}_0^1 \cdot \frac{d\mathbf{f}_1}{dv} \\
&\quad + \frac{\partial \mathbf{f}_M}{\partial v}, \\
\mathbf{M}_1 \cdot \frac{d\mathbf{f}_1}{dv} &= (\mathbf{E}_1^2 - \mathbf{D}_1) \cdot \left( \mathbf{f}_0^n + \Delta v \frac{d\mathbf{f}_0}{dv} \right) + \mathbf{E}_1^1 \cdot \frac{d\mathbf{f}_0}{dv} \\
&\quad + (\mathbf{B} + \mathbf{M}_1^t) \cdot \left( \mathbf{f}_1^n + \Delta v \frac{d\mathbf{f}_1}{dv} \right),
\end{aligned}$$

$$\frac{d\mathbf{f}_0}{dv} = \tilde{\mathbf{A}}_0 \cdot \frac{d\mathbf{f}_1}{dv} + \mathbf{b}_0 \left( \mathbf{f}_1^n, \frac{\partial \mathbf{f}_M}{\partial v} \right), \quad (27)$$

$$(\mathbf{M}_1 - \Delta v (\mathbf{B} + \mathbf{M}_1^t)) \cdot \frac{d\mathbf{f}_1}{dv} = \tilde{\mathbf{A}}_1 \cdot \frac{d\mathbf{f}_0}{dv} + \mathbf{b}_1 (\mathbf{f}_1^n, \mathbf{f}_0^n), \quad (28)$$

$$(\mathbf{M}_1 - \Delta v (\mathbf{B} + \mathbf{M}_1^t) - \tilde{\mathbf{A}}_1 \cdot \tilde{\mathbf{A}}_0) \cdot \frac{d\mathbf{f}_1}{dv} = \tilde{\mathbf{A}}_1 \cdot \mathbf{b}_0 + \mathbf{b}_1, \quad (29)$$



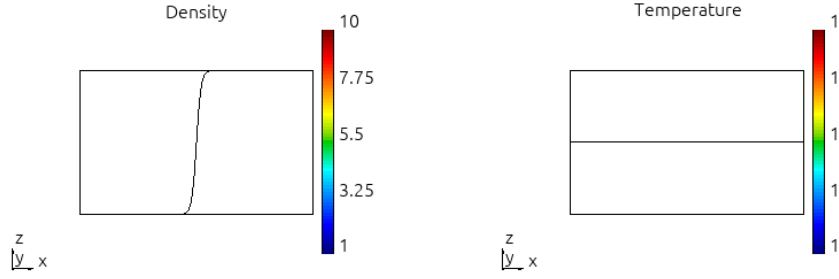


Figure 2: Problem 4 background.

50 [2]

## References

- [1] J. R. Albritton, E. A. Williams, I. B. Bernstein, Nonlocal electron heat transport by not quite maxwell-boltzmann distributions, *Phys. Rev. Lett.* 57 (1986) 1887–1890.
- 55 [2] V. Dobrev, T. Kolev, R. Rieben, High-order curvilinear finite element methods for Lagrangian hydrodynamics, *SIAM J. Sci. Comput.* 34 (2012) B606–B641.

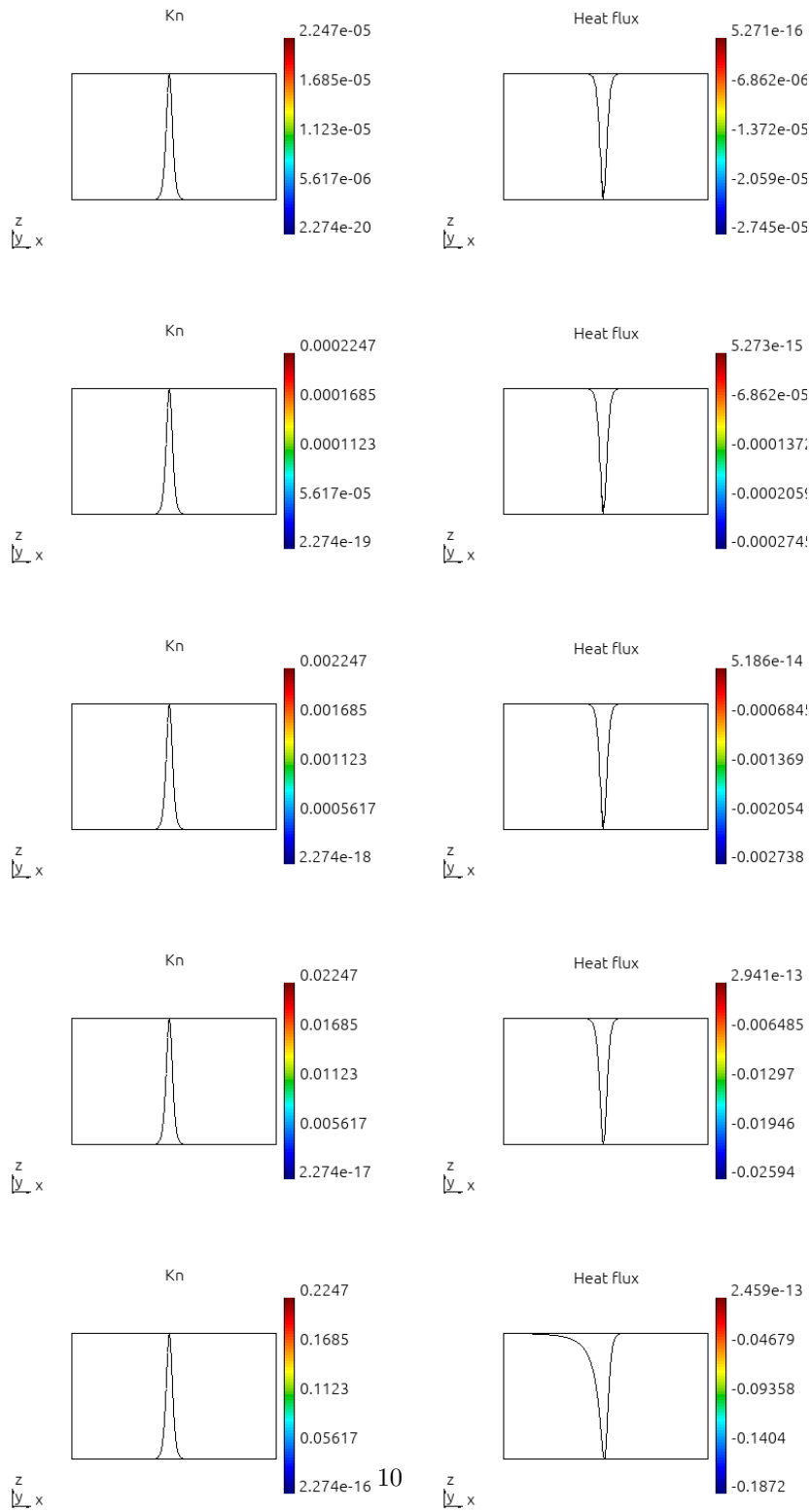


Figure 3: Problem 4 transport.

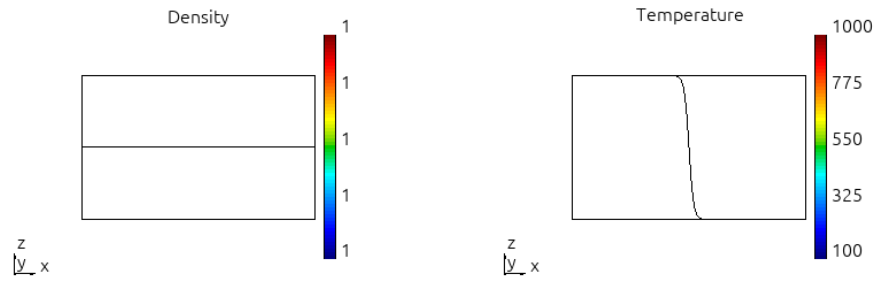


Figure 4: VFP-paper corresponding simulations, ion background density and temperature.

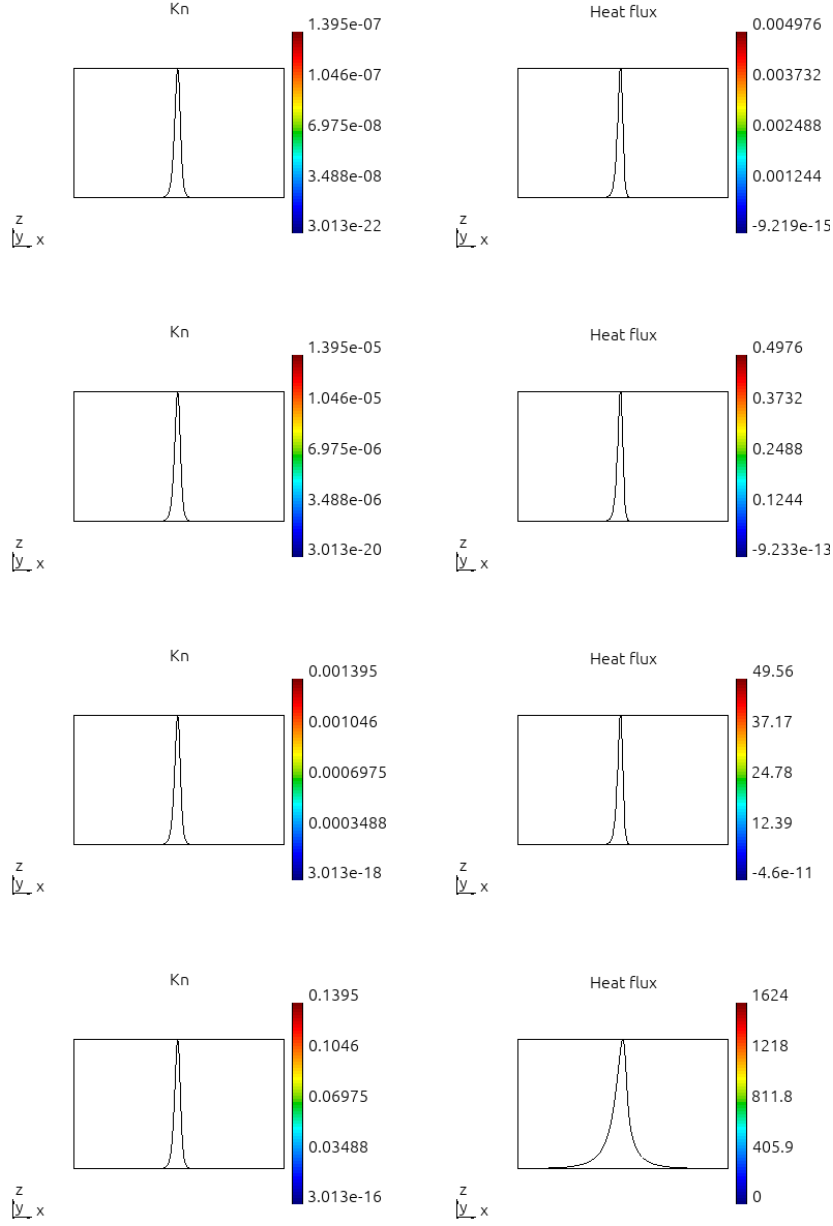


Figure 5: VFP-paper corresponding simulations, Kn spans the interval ( $\approx 10^{-7}, \approx 10^{-1}$ ) where flux goes from diffusive to highly nonlocal.

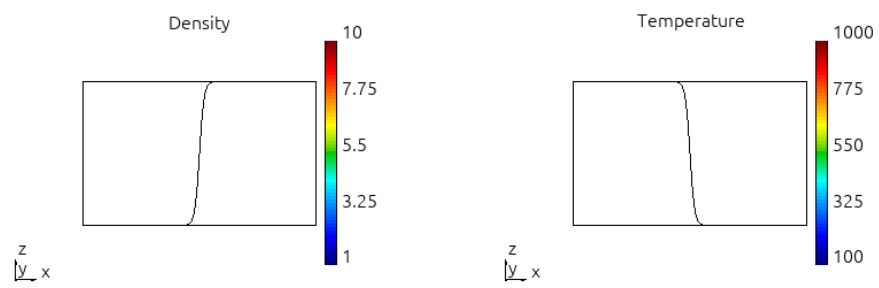


Figure 6: Problem 6 background.

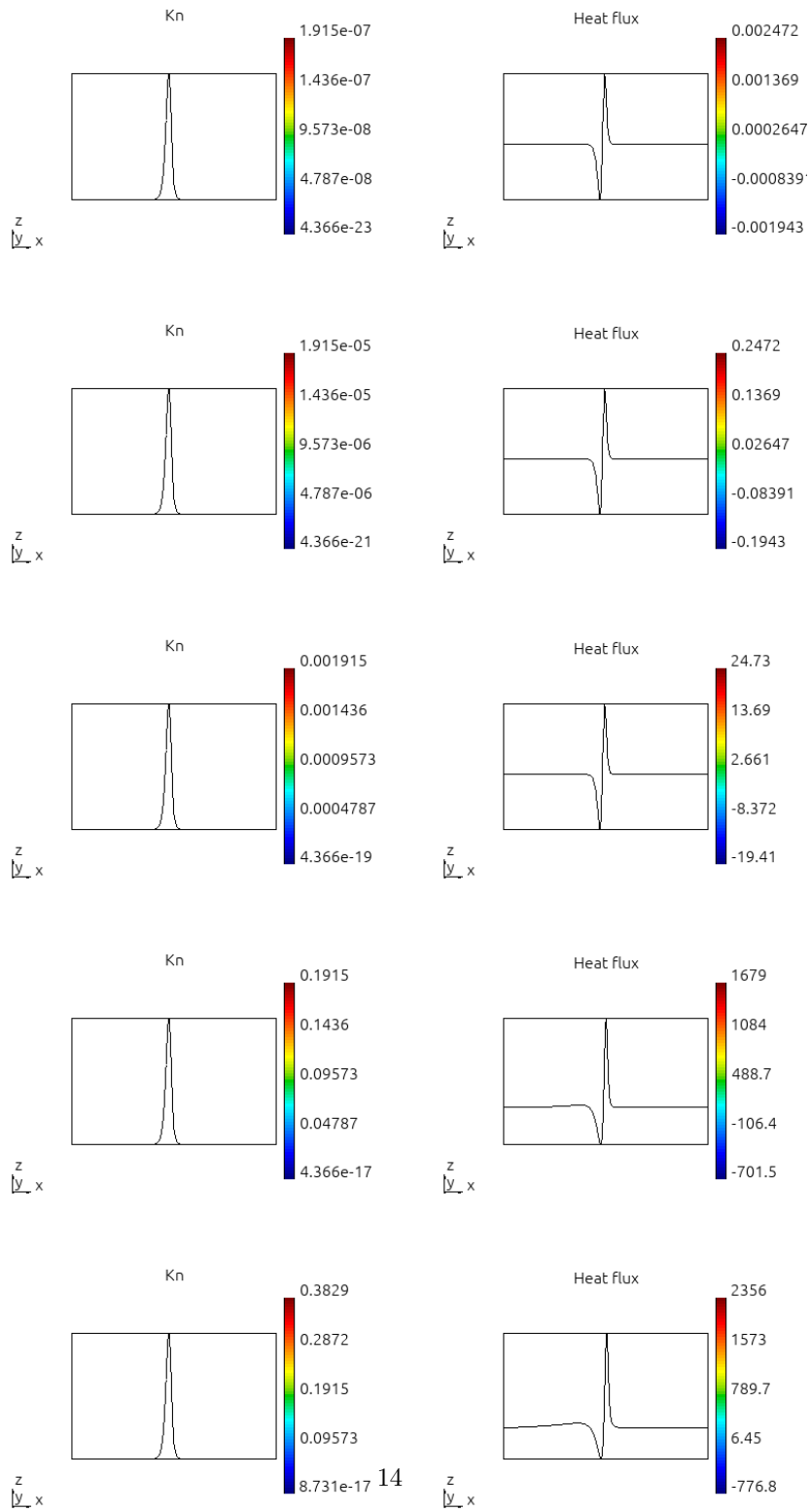


Figure 7: Problem 6 transport.

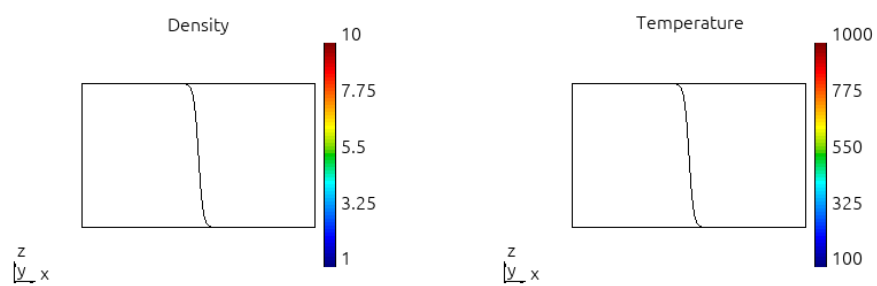


Figure 8: Problem 7 background.

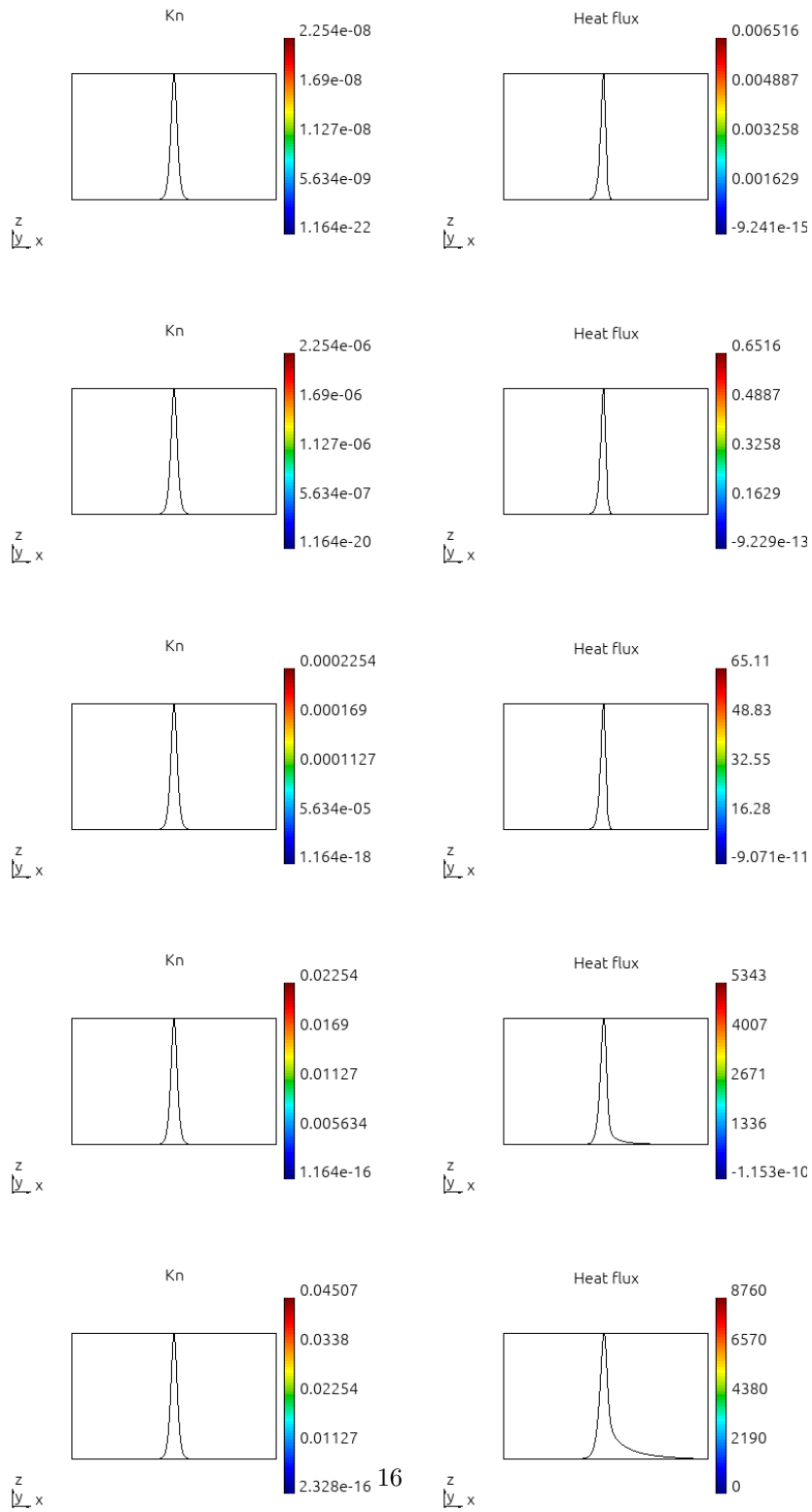


Figure 9: Problem 7 transport.



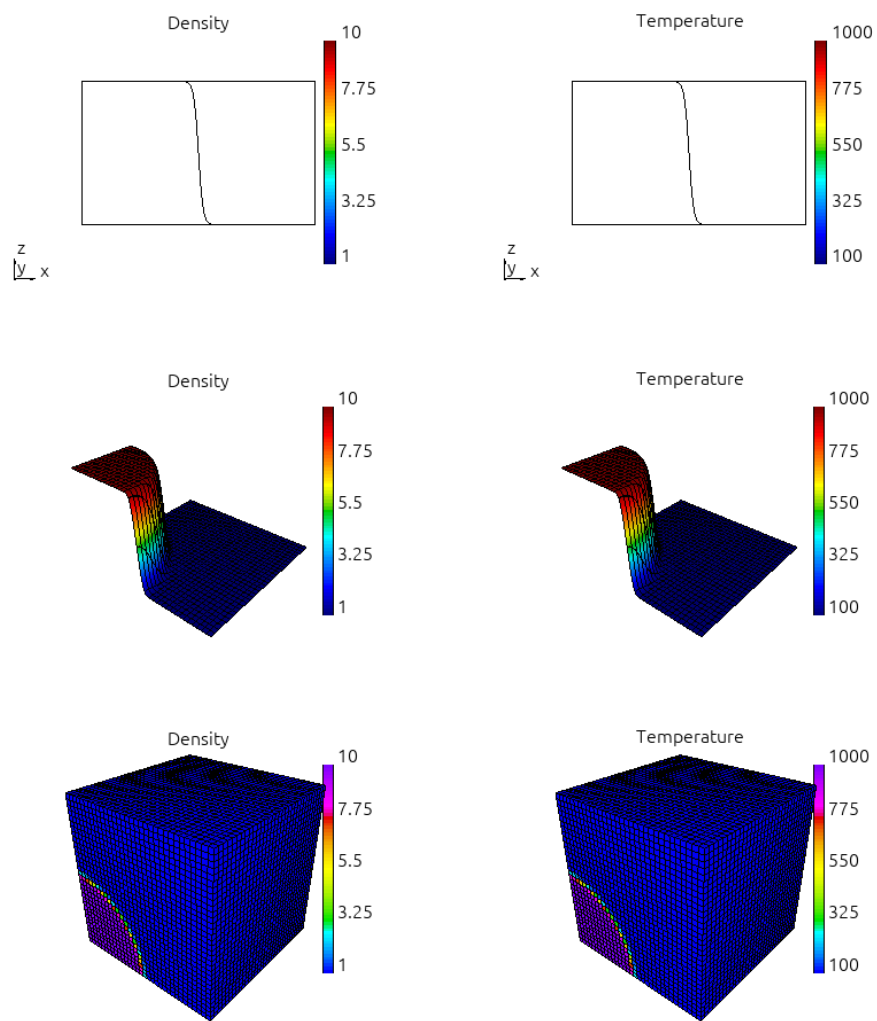


Figure 10: Problem 7 1D/2D/3D background.

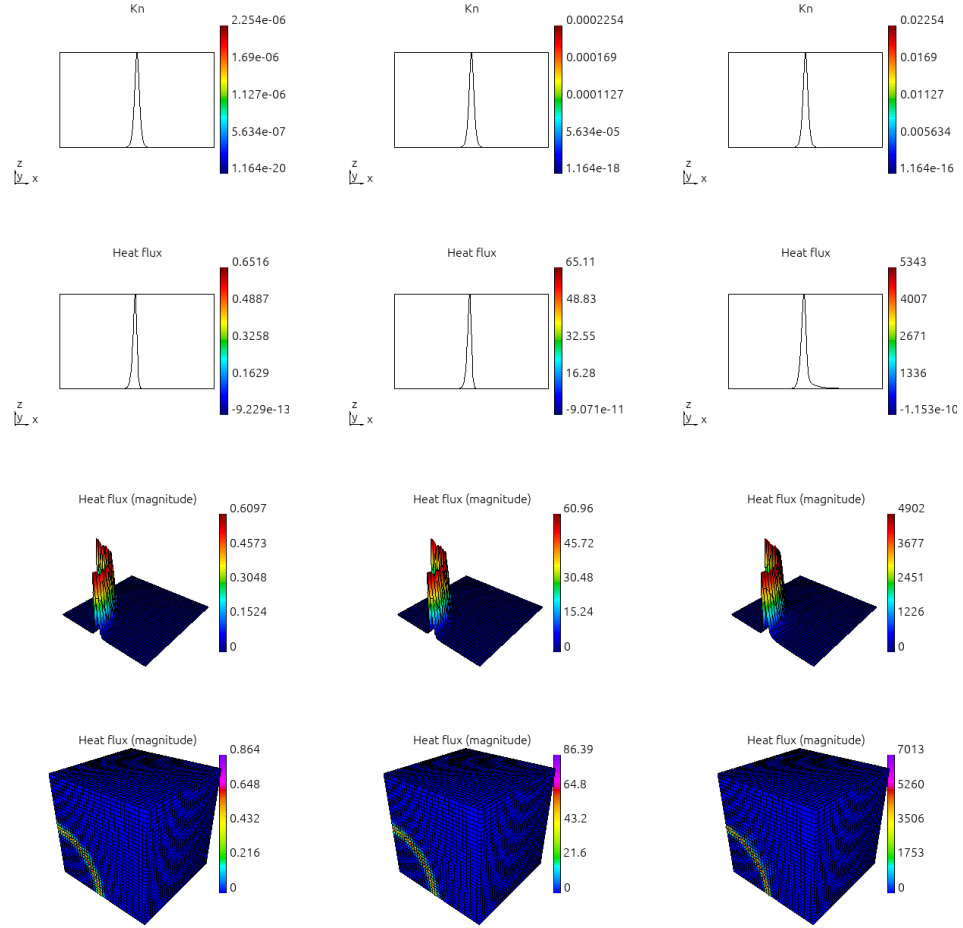


Figure 11: Problem 7 1D/2D/3D transport.

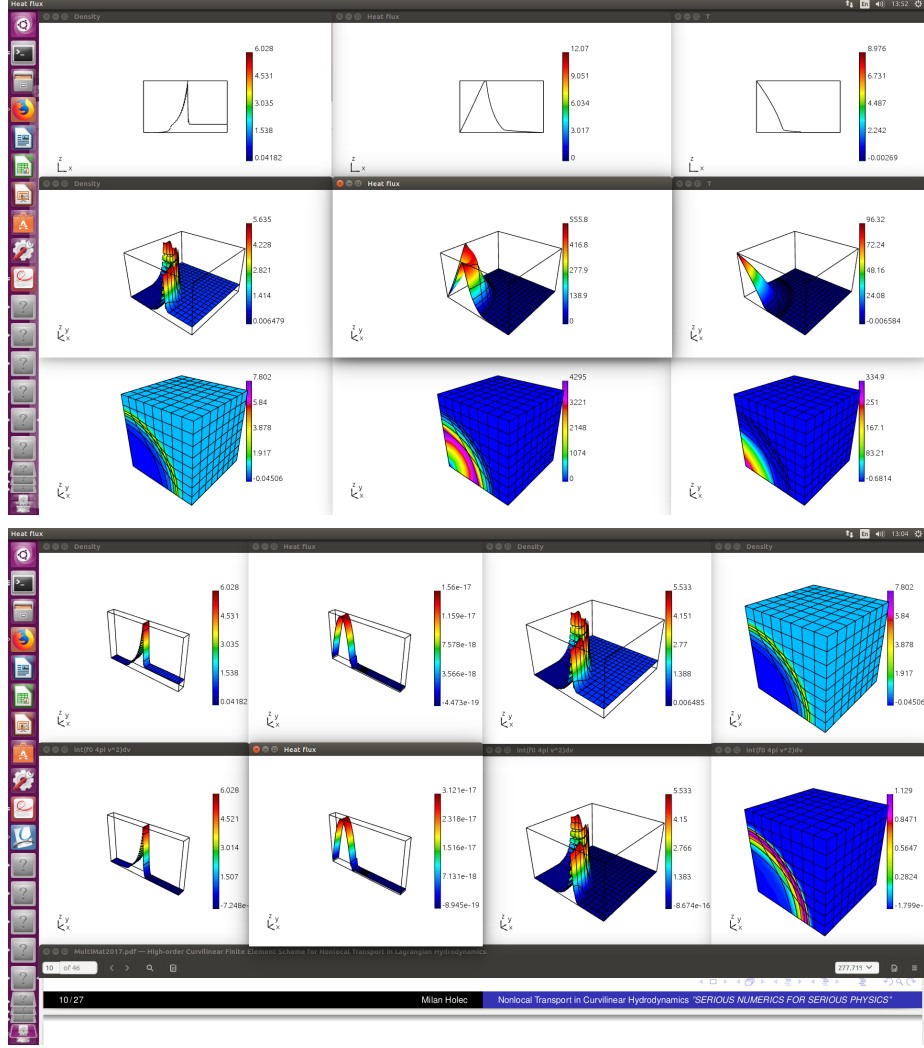


Figure 12: Sedov blast in 1D/2D/3D from  $\delta$  function hot spot. Shock propagates from left to right. Top row corresponds to 1D (8858 energy groups) - left: density profile, right: temperature (decreasing from the original hot spot with low temperature in compressed plasma), center: heat flux with its maximum on the start of increase in density decreasing while approaching the shock (NOTICE non-zero flux ahead of the shock). Middle row corresponds to 2D (4348 energy groups) - left: density, center: heat flux, right: temperature. Bottom row corresponds to 3D (10030 energy groups) - left: density, center: heat flux, right: temperature.